Understanding Polymer-Cell Attachment

DOI: 10.1002/marc.((insert number)) ((or ppap., mabi., macp., mame., mren., mats.))

Article Type (Full Paper)

Understanding Polymer-Cell Attachment

Andrea Venturato, Gillian MacFarlane, Jin Geng* and Mark Bradley*

A Venturato, G. MacFarlane, Dr. J. Geng, Prof. M Bradley
School of Chemistry, University of Edinburgh, The King's Buildings, West Mains Road, Edinburgh, UK EH9 3KJ
E-mail: jin.geng@ed.ac.uk; Mark.Bradley@ed.ac.uk

The development of polymeric materials with cell adhesion abilities requires an understanding of cell–surface interactions which vary with cell type. To investigate the correlation between cell attachment and the nature of the polymer, a series of random and block copolymers composed of dimethyl amino ethyl acrylate and ethyl acrylate were synthesized through single electron transfer living radical polymerization. The polymers were synthesized with highly defined and controlled monomer compositions and exhibited narrow polydispersity indices (PDI)s. These polymers were examined for their performance in the attachment and growth of HeLa and HEK cells, with attachment successfully modeled on monomer composition and polymer chain length, with both cell lines found to preferentially attach to moderately hydrophobic functional materials. The understanding of the biological-material interactions assessed in this study will underpin further investigations of engineered polymer scaffolds with predictable cell binding performance.

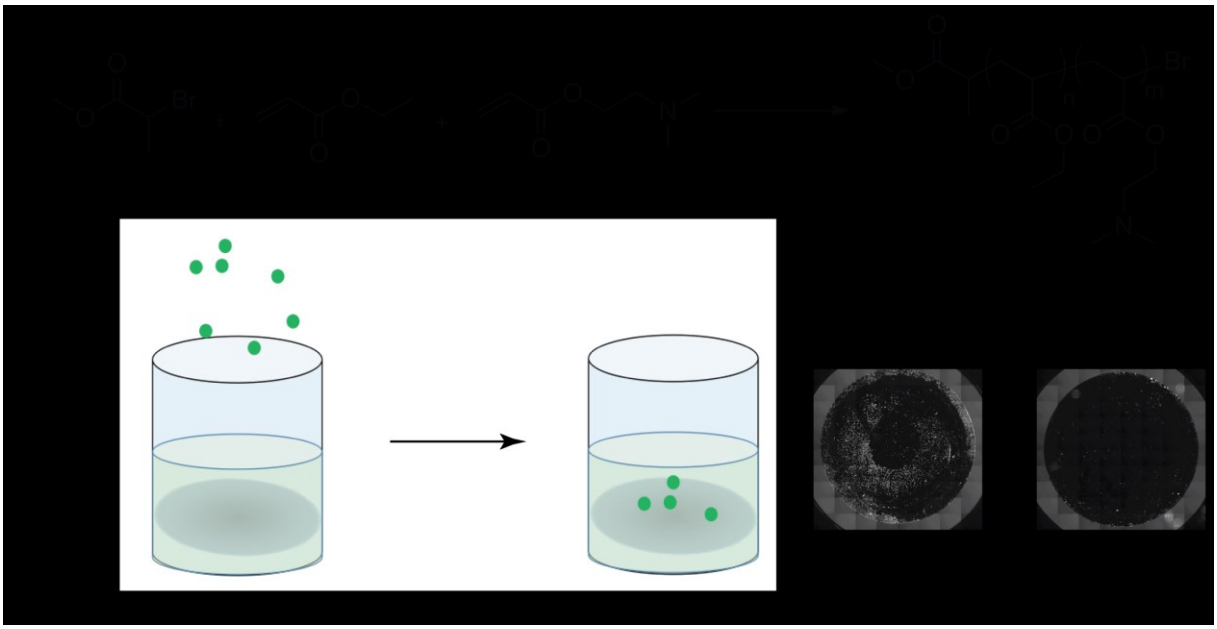

1. Introduction

Polymers have been extensively studied as substrates for cell culture,[1-5] with the development of high-throughput polymer based microarrays enabling the simultaneous screening of thousands of different polymeric materials with different mechanical and chemical properties.[6,7] High-throughput approaches have led to the discovery of biomaterials with potential applications in different fields (i.e. substrates for control of stem cell culture,[8-11] platelet activation[12] and stabilization of hESC derived functional hepatocytes[13]). Differential cell adhesion has previously been shown to be based upon a materials' chemical, physical and mechanical properties,[14-16] with the broadly accepted first steps of the mechanism of cell attachment onto polymer surfaces being the adsorption of proteins onto a polymer with this "hard attachment" (or corona) followed by a more dynamic "softer" layer, with interactions between cells and these proteins.[17,18] A number of theories have been developed to explain this process of cell-adhesion with the goal of establishing a predictive basis for cell binding, and to explain how the sub-stratum surface properties so profoundly affect cell-material

interactions and cellular differentiation.[6,19-21] Factors such as material topography,[22,23] surface wettability,[24,25] free energy,[26] surface stiffness entwined with surface chemistry play a key role in the cell adhesion mechanism as well as influence cell behavior and differentiation. The control of such chemical and physical properties is a critical point which needs to be addressed to allow a better understanding to be obtained and allow finer control of cell-material interactions. This would be translated into the ability to develop materials that are able to achieve specific biological functions, such as the control of proliferation or differentiation, whilst clarifying our understanding of polymer cell-binding properties.[27] The chemical composition of the substrate is fundamental for correct protein adsorption onto the materials surface. Block copolymers represent an interesting approach to the modulation of chemical surface due to their ability to form chemically different polymer segments and to self-assemble generating nano-scale morphologies.[28,29] Despite block copolymers having interesting properties and the potential to be used for the tuning of synthetic substrates' surface, limited work has been done to explore the possible surface-cell interaction.[30]

Thus here a small library of highly defined, well-characterized polymers was synthesized based on two different monomers with varying monomer composition, polymer structure, and chain length. Single-electron transfer living radical polymerization (SET-LRP) has been used to produce well-defined polymers using a number of different monomers including acrylates, acrylamides and methacrylates and co and multi-block copolymers with complete monomer conversion.[31-33] In order to generate polymers that could be used in such a systematic study, SET-LRP was explored using the monomers dimethylamino ethyl acrylate (DMAEA) and ethyl acrylate (EA) (as these have previously been shown to interact with cells[34]) with all polymers purified and characterized by gel permeation chromatography (GPC) and nuclear magnetic resonance (NMR).

2. Experimental Section

2.1. Materials

2-Bromo-2-methyl-propionic acid benzyl ester initiator was synthesized as previous described.[35] Ethyl acrylate (EA) (99%, Acros) and dimethylamino ethyl acrylate (DMAEA) (98%, Sigma-Aldrich) was passed over a short-column of basic Al_2O_3 before use in order to remove the radical inhibitor. NMR experiments were carried out on a Brüker Pro500 spectrometer. Molar mass distributions were measured by size exclusion chromatography (SEC), on a system equipped with two Polymer Laboratory GPC columns (PL gel 5 μm mixed D-columns, 300 x 7.5 mm) and one PL gel 5 μm guard column (50 x 7.5 mm) (Polymer Laboratories, suitable for molecular weights between 200 and 400,000 g mol^{-1}) with differential refractive index detection using N, N-dimethylformamide (DMF) / 0.1M LiBr at 1 mL min^{-1} as the eluent with the temperature set at 60 ºC. Poly(MMA) standards were used to calibrate the SEC. Cell imaging was carried out on a Zeiss semi-confocal microscope, with cell culture reagents purchased from Invitrogen unless otherwise stated.

2.2. Polymerizations

The polymerizations were carried out using the same monomers, initiator and ligand with the amounts of each monomer varied for each polymerization (see supporting information). Dimethylamino ethyl acrylate (DMAEA) (1.0 ml, 6.58 mmol), ethyl acrylate (EA) (0.35 ml, 3.30 mmol), initiator (14.6 μl, 0.131 mmol), Me_6TREN (7.0 μl, 0.0263 mmol), and DMSO (1 ml) were added to a Schlenk flask and degassed under nitrogen for 30 minutes. 10 cm of copper wire (20 gauge wire, 0.812 mm diameter, Fischer) was placed in 2,2,2-trifluoroethanol (TFE, 2

ml (>99%, Alfa-Aesar) degassed) and left for 30 minutes according to the method of Haddleton.[33] The copper wire was washed with THF and ethanol, dried under vacuum for 10 minutes, and added to the reaction flask (with the monomer and initiator) and left for 4 hours. To precipitate the polymer, the solution was firstly dissolved in THF and then filtered through a basic aluminium oxide column to remove traces of copper. The polymer was precipitated from the solution by the addition of water/ethanol (1:2) and the polymer recovered by centrifugation and dried in a vacuum oven overnight. For sampling for conversion, a degassed syringe was used to remove a droplet of reaction mixture every 30 minutes over the 4 hours reaction period and the consumption of monomer was measured via NMR. The conversion was calculated by comparison between the signal relative to the C=CH_2 protons of the monomer (singlet, 5.5 ppm or 6.0 ppm, decreasing with time) and those of analogous C(O)OCH_2 proton of the polymer repeating unit (broad singlet, 4.1 ppm, increasing with time).

2.3. Block Copolymerization

EA (1.0 ml, 6.58 mol), initiator (14.6 µl, 0.131 mmol), Me_6TREN (7.0 µl, 0.0263 mmol), and DMSO (1 ml) were added to a Schlenk flask and degassed under nitrogen for 30 minutes. The polymerization was carried out as described above. Once conversion was > 99%, DMAEA (1.0 ml, 6.58 mmol) in degassed DMSO (0.5 mL) and added to the reaction mixture. A sample was taken as a starting measurement for comparison of the 2 monomers. To precipitate the polymer, the solution was diluted with THF and then filtered through basic aluminum oxide column to remove traces of copper. This filtered solution was then precipitated into water/ethanol (1:2). The solution was then centrifuged and the liquid was decanted leaving a pellet of polymer. The product was dried in a vacuum oven overnight.

2.4. Coverslip Fabrication

Coated coverslips (8 mm in diameter) were prepared as follows: (i). Polymer was dissolved in THF to give a final concentration of 2 % (w/v); (ii). 30 µl of each polymer solution was spotted onto the center of the coverslips and spin coated for 3 second at 2000 rpm (Spin Coater p6700, Specialty Coating Systems); (iii). Coverslips were dried overnight in oven at 40 ºC; (iv). Dried coverslips were placed into a 48 well-plate and stored for future. For each polymer 6 coverslips were fabricated.

For contact angle assessment 13 mm and 18 mm coverslips were spin-coated with polymer (in THF at 2% (w/v)), using 0.17 µl/mm^2.

2.5. Characterisation

Advancing contact angles of distilled water were measured with a Krüss goniometer (model G10). The experiment was performed under ambient conditions with the needle tip in contact with the drop. For each polymer sample three coated coverslips were tested, on each coverslip 3 water drops were dispensed in different positions (central and edges of the coverslip) and contact angle was recorded. Images of the drops on coverslips were taken using a USB Digital Microscope BP-M8400 placed vertically to the coverslip surface. Once the images were recorded, they were processed using the ImageJ to calculate the area of each drop area.

2.6. Cell Culture

HeLa and HEK cells were grown in 25 cm^2 tissue culture flasks (Corning) in DMEM supplemented with 10% FCS (BIOSERA FB-1090/500), L-glut (100 units, Ml Gibco 25030-024) and pen/strep (100 units/mL, Sigma P4333), and incubated at 37 °C with 5% CO_2. Cells were passaged every 2 days. Cells were detached using Trypsin, spun down at 1500 rpm for 5

min, the supernatant discarded, and the cells re-suspended in DMEM (2 mL) with 10% FCS. 10 µl of cell suspension were added to 30 µl of Trypan Blue; from this solutions 10 µl were collected and placed on a counting chamber. Cell counting was performed twice for each cell population. 48 well-plates containing 3 coverslips of each polymer for each cell-line were sterilized under UV irradiation for 30 min. 30000 cells of each cell-line were seeded in triplicate for each polymer and DMEM supplemented media was added to give a final volume of 500 µl/well. 48 well-plates were incubated for 24h (37 °C with 5% CO_2), the coverslips were washed with PBS, fixed with 4% formaldehyde in PBS for 10 min, washed twice with PBS and incubated with DAPI (1 µg/ml) for 15 min, followed by two washing with PBS.

2.7. Imaging and Analysis

Coverslips were imaged in the DAPI and Bright-field channels using a Zeiss semi-confocal microscope using a 10X magnification objective. For each coverslip a mosaic of images (9x9, 9409x9217 pixel) were captured. Images were merged and saved as TIF format files for image analysis purposes. Image analysis was performed using ImageJ with ITCN cell counting plugin. On each mosaic picture (9x9), coverslip area was identified and cell nuclei into the area were counted. Nuclei diameter was established as a width of 7 pixels; a minimum distance between nuclei was set to 2.5 pixels with a threshold of 2.0. These parameters allow the identification of nuclei and the counting of single nuclei when cells are present in clusters.

Based on cell number average cell binding density per polymer was calculated. For each polymer standard deviation (n=3) was calculated.

3. Results and Discussion

3.1. Polymer synthesis

Random and block copolymers were prepared with varying compositions of the monomers dimethyl amino ethyl acrylate and ethyl acrylate using SET-LRP. In order for the polymers to be part of this study, they were first characterized to fully confirm their desired structure and end chain functionality. Due to the controlled nature of the polymerization method, the end chain functionalities of the polymers were defined, being derived from the initiator used (Scheme 1). Table 1 shows the different copolymers synthesized with the corresponding composition, molecular weights and PDI's. Well defined random and block co-polymers with M_n up to 100 KDa with narrow molecular weight distributions were generated. The kinetic plots for the co-polymerization of DMAEA and EA was linear. As expected as the monomer was consumed the M_n of the copolymer increased whilst the PDI remained relatively narrow (Figure 1 shows the synthesis/analysis of P5 as an example). The composition of the polymer was calculated from the ^{1}H NMR spectrum comparing the integrals of the initiator/end group (~3.6 ppm) and the CH_2- groups next to ester group (~4.2 ppm), giving n + m. The number of DMAEA, m was calculated using integral of Me_2N- group compared with the initiator/end group. The molecular weights (M_n) of the polymers were calculated based on the monomer composition. The proton NMR spectra of P1, P5 and P6 are shown in Figure 2.

3.2. Preparation of polymer surface for cellular attachment

The polymers coated glass coverslips were used in this cellular attachment study. HeLa and HEK cells were seeded onto the coverslips, and incubated for 24 hours After stained with DAPI (4',6-diamidino-2-phenylindole), each entire coverslip was imaged, taking a 9 × 9 mosaic in order to cover the whole area (in Figure 3a and 3b showing the integrated images). It was clearly seen that there were different proportions of surface covering by cells (in white DAPI nuclei staining) on different polymers.

Images were used to calculate cell number on each coverslip using ImageJ, with cell number and cell density for each coverslip determined via Image-based Tool for Counting Nuclei.[36] The cell densities are shown in Table 2. For all the polymers analyzed HEK cell number was greater than HeLa due to differences in their proliferation rates, with major differences observed in cell number and monomer composition (Figure 4). The hydrophobic EA (P15) homo-polymer was found have the highest cell density of both HEK (421 mm^{-2}) and HeLa cells (256 mm^{-2}). When comparing the images of cell attachment and SEM images of the surface of polymer coated coverslip, Figure 3c and 3d, we found that cellular attachment may relate to the surface topological differences resulting in spin-coating. It was also observed that some polymers promoted clumping, while other polymers had a more even distribution of the cells across the whole surface (see Figure 3e and 3f).

3.3. How polymer properties affect cellular attachment

Comparing all polymers and looking at cell attachment, showed only a weak/no trend of cell attachment and monomer composition. However, if random and block copolymer were analyzed separately, a trend was observed which showed that as the percentage of DMAEA in the copolymers increased, HEK and HeLa cell number decreased (Figure 5). It indicated that the copolymers with the higher EA gave a better surface for supporting cell growth regardless of the way in which the monomers were dispersed along the polymer chain.

A comparison of the block copolymers and the random copolymers showed that there was a difference in cell number with the different types of polymerization method. Noticeably, when there was a greater content of EA, the random copolymer had a greater cell number when compared to the block copolymer of the same composition, such as P10 and BP2 which resulted in very different cell densities, 626 and 118 respectively. On the other hand, when the DMAEA content was higher than or equal to that of the EA content, the block copolymer displayed a

higher cell number compared to the random copolymer with an identical of the corresponding monomer composition. This suggests that for block and random copolymers with high concentrations of DMAEA (> 50%) but similar molecular weights, cell binding seems to be highly influenced by DMAEA organization (the measured contact angles of random and block copolymers for example P10 and BP2 were respectively 10.67 and 54.67) which will thus interact with cells via the polymer surface in different ways. Previous work has shown that block copolymers form distinct morphologies through phase separation and have a significant influence on the protein adsorption to the polymer surface.[37-39] Other reported work has also highlighted how the grouping of the different functionalities on the polymer chains of block copolymers affect protein adsorption and eventually cell adhesion on the surface.[30,40-42]

Polymer molecular weights were plotted in relation to the cell numbers for both HeLa and HEK cells for the random and block copolymers. Figure 4c showed a clear trend of cell numbers for both cell lines. There was a clear increase in cell number with increasing molecular weight of the copolymers with molecular weight in the range of 2 kDa to 40 kDa. This trend was similar for both cell lines though the increase seen for the HEK cell line was more evident than that observed for HeLa. In addition, cell numbers were plotted in relation to both the monomer ratio and polymer molecular weight, as seen in Figure 5d and 5e. When comparing the polymers that have similar monomer ratios, the ones with longer polymeric chain have greater cell numbers.

3.4. How surface property affect cellular attachment

To further investigate the relation between cells and the material surface contact angle and spreading area were assessed on polymer coated coverslips.

Most of the polymer had a droplet contact angle between 30 to 50 degrees, which is in the optimal range for protein adsorption (Table S2).[38] Samples P14, P4 and P8 had large standard deviation compared to other polymers, presumably attributable to the coating topography being

a non-homogeneous layer. As previously described in images 3C and 3D, the difference in topography on the same coverslips affects droplet behavior on the surface and thus influence the final contact values. Wetting of the surface was also measured imaging droplets after they spread onto polymer surface, then area of each drop was calculated and plotted against contact angle for the same drop. The majority of the samples resulted in partial wetting ($\theta < 70°$) with some polymers showing total wetting ($\theta < 20°$). Overall, block copolymers had a higher contact angle when compared with the random copolymer with similar compositions of EA and DMAEA % (Figure 6). A minimal trend was observed when comparing contact angle and concentration of EA. A higher contact angle was observed when the percentage of EA was higher than 50%, in accordance with the increasing hydrophobicity of the polymer. A good correlation was obtained between spreading area of the droplet and the angle measured (Figure 7) further confirming the polymer surface properties and allowing us in future to tune polymer chain composition in relation to the material surface properties.[21]

4. Conclusions

In conclusion, a small polymer library was used to screen for materials that support the attachment of HeLa and HEK cells. The synthesis of random and block copolymers using only two monomers, DMAEA and EA, was achieved using a controlled method of polymerization, single-electron transfer living radical polymerization. The polymers were tested for cell growth and showed that all the copolymers prepared were able to support cell growths, importantly there was a noticeable difference in cell attachment observed when the monomer composition and polymer chain length were varied. Both the random and block copolymers with a higher EA content were more favorable for both HeLa and HEK cell attachment. The polymers surface chemistries were characterized by contact angle measurements and displaying a range from 20 to 70 degree. Increasing concentration of EA resulted in a higher contact angle. Overall, block

copolymers displayed higher contact angles than the analogous random copolymers. Further work will be carried out to investigate how phase separated block copolymers on surfaces control protein ordering/binding and subsequent and cell culture.

A clearer correlation between HeLa cell attachment and monomer composition for block copolymer was observed, suggesting cell binds was influenced by the material's properties that are not determined by composition but rather from the method of synthesis. We are currently developing strategies for polymer microarrays through controlled living radical polymerization, which should allow us to establish a full polymer library with a wide range of well-defined structures. These insights develop the understanding of the correlation of cell interaction and polymer structure and will underpin the development of method in preparation of cell-materials.

References

[1] H. Shin, S. Jo, A. G. Mikos, *Biomaterials* **2003**, *24*, 4353–4364.

[2] F. Khan, R. S. Tare, J. M. Kanczler, R. O. C. Oreffo, M. Bradley, *Biomaterials* **2010**, *31*, 2216–2228.

[3] S. Pernagallo, O. Tura, M. Wu, K. Samuel, J. J. Díaz-Mochón, A. Hansen, R. Zhang, M. Jackson, G. J. Padfield, P. W. F. Hadoke, et al., *Adv Healthc Mater* **2012**, *1*, 646–656.

[4] A. Mant, G. Tourniaire, J. J. Díaz-Mochón, T. J. Elliott, A. P. Williams, M. Bradley, *Biomaterials* **2006**, *27*, 5299–5306.

[5] A. Hansen, S. Corless, A. Cleland, J. Petrik, N. Gilbert, M. Bradley, *Macromol Biosci* **2013**, *13*, 437–443.

[6] D. G. Anderson, S. Levenberg, R. Langer, *Nat Biotechnol* **2004**, *22*, 863–866.

[7] H. Mizomoto, Ph.D. Thesis, University of Southampton, **2004**.

[8] A. Hansen, H. K. Mjoseng, R. Zhang, M. Kalloudis, V. Koutsos, P. A. de Sousa, M. Bradley, *Adv Healthc Mater* **2014**, *3*, 848–853.

[9] C. Mangani, A. Lilienkampf, M. Roy, P. A. de Sousa, M. Bradley, *Biomater Sci* **2015**, *3*, 1371–1375.

[10] C. R. E. Duffy, R. Zhang, S.-E. How, A. Lilienkampf, P. A. de Sousa, M. Bradley, *Biomaterials* **2014**, *35*, 5998–6005.

[11] R. Zhang, H. K. Mjoseng, M. A. Hoeve, N. G. Bauer, S. Pells, R. Besseling, S. Velugotla, G. Tourniaire, R. E. B. Kishen, Y. Tsenkina, et al., *Nat Comms* **2013**, *4*, 1335.

[12] A. Hansen, L. McMillan, A. Morrison, J. Petrik, M. Bradley, *Biomaterials* **2011**, *32*, 7034–7041.

[13] D. C. Hay, S. Pernagallo, J. J. Díaz-Mochón, C. N. Medine, S. Greenhough, Z. Hannoun, J. Schrader, J. R. Black, J. Fletcher, D. Dalgetty, et al., *Stem Cell Res* **2011**, *6*, 92–102.

[14] C.-M. Lo, H.-B. Wang, M. Dembo, Y.-L. Wang, *Biophys J* **2000**, *79*, 144–152.

[15] D. E. Discher, P. Janmey, Y.-L. Wang, *Science* **2005**, *310*, 1139–1143.

[16] C. R. E. Duffy, R. Zhang, S.-E. How, A. Lilienkampf, G. Tourniaire, W. Hu, C. C.

West, P. de Sousa, M. Bradley, *Biomater Sci* **2014**, *2*, 1683–1692.
[17] J. R. Klim, L. Li, P. J. Wrighton, M. S. Piekarczyk, L. L. Kiessling, *Nat Methods* **2010**, *7*, 989–994.
[18] Y. Meng, S. Eshghi, Y. J. Li, R. Schmidt, D. V. Schaffer, K. E. Healy, *FASEB J* **2010**, *24*, 1056–1065.
[19] G. Tourniaire, J. Collins, S. Campbell, H. Mizomoto, S. Ogawa, J.-F. Thaburet, M. Bradley, *Chem Comm* **2006**, *0*, 2118–2120.
[20] S. E. How, B. Yingyongnarongkul, M. A. Fara, J. J. Díaz-Mochón, S. Mittoo, M. Bradley, *Comb Chem High T Scr* **2004**, *7*, 423–430.
[21] J.-F. Thaburet, H. Mizomoto, M. Bradley, *Macromol Rapid Comm* **2004**, *25*, 366–370.
[22] M. J. Dalby, N. Gadegaard, R. O. C. Oreffo, *Nat Mater* **2014**, *13*, 558–569.
[23] M. H. Kim, Y. Sawada, M. Taya, *J Biol Eng* **2014**, 1–9.
[24] S. J. Lee, G. Khang, Y. M. Lee, H. B. Lee, *J Colloid Interf Sci* **2003**, *259*, 228–235.
[25] J. H. Lee, G. Khang, J. W. Lee, H. B. Lee, *J Colloid Interf Sci* **1998**, *205*, 323–330.
[26] K. Ishihara, T. Kitagawa, Y. Inoue, *ACS Biomater. Sci. Eng.* **2015**, *1*, 103–109.
[27] L. M. Szott, T. A. Horbett, *Curr Opin Chem Biol* **2011**, *15*, 677–682.
[28] I. W. Hamley, *Prog Polym Sci* **2009**, *34*, 1161–1210.
[29] Alioscka Sousa, Merih Sengonul, Robert Latour, A. Joachim Kohn, M. Libera, *Langmuir* **2006**, *22*, 6286–6292.
[30] J.-H. Seo, R. Matsuno, M. Takai, K. Ishihara, *Biomaterials* **2009**, *30*, 5330–5340.
[31] F. Alsubaie, A. Anastasaki, P. Wilson, D. M. Haddleton, *Polym Chem* **2015**, *6*, 406–417.
[32] S. R. Samanta, V. Percec, *Polym Chem* **2014**, *5*, 169–174.
[33] S. R. Samanta, V. Nikolaou, S. Keller, M. J. Monteiro, D. A. Wilson, D. M. Haddleton, V. Percec, *Polym Chem* **2015**, *6*, 2084–2097.
[34] A. H. Soeriyadi, C. Boyer, F. Nyström, P. B. Zetterlund, M. R. Whittaker, *J Am Chem Soc* **2011**, *133*, 11128–11131.
[35] Neldes J Hovestad, Gerard van Koten, A. Stefan A F Bon, David M Haddleton, *Macromolecules* **2000**, *33*, 4048–4052.
[36] L. L. Drey, M. C. Graber, J. Bieschke, *BioTechniques* **2013**, *55*, 28–33.
[37] M. Palacio, S. Schricker, B. Bhushan, *J. Microsc.* **2010**, *240*, 239–248.
[38] P. Viswanathan, E. Themistou, K. Ngamkham, G. C. Reilly, S. P. Armes, G. Battaglia, *Biomacromolecules* **2014**, *16*, 66–75.
[39] S. R. Schricker, M. L. B. Palacio, B. Bhushan, *Colloid Polym Sci* **2011**, *289*, 219–225.
[40] D. V. Bax, A. Kondyurin, A. Waterhouse, D. R. McKenzie, A. S. Weiss, M. M. M. Bilek, *Biomaterials* **2014**, *35*, 6797–6809.
[41] G. Yu, J. Ji, H. Zhu, J. Shen, *J. Biomed. Mater. Res. Part B Appl. Biomater* **2006**, 76B: 64–75.
[42] B. Cao, S. Yan, K. Zhang, Z. Song, T. Cao, X. Chen, L. Cui, J. Yin, *Macromol Biosci* **2011**, *11*, 970–977.

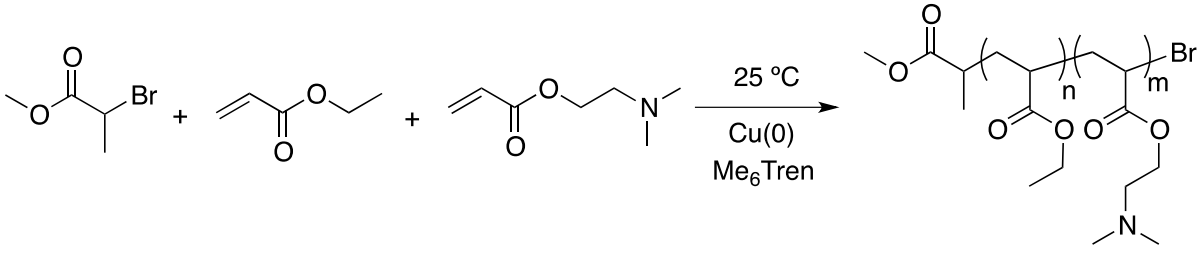

Scheme 1. Co-polymerization of DMAEA and EA via SET-LRP.

Table 1. Polymers synthesized in this study: [a]Monomer ratio calculated from NMR; [b]determined by GPC. Note: P1-P13 are random copolymers, P14 and P15 are homopolymers, BP1-BP5 are block copolymers.

Polymer	DMAEA(m)[a]	EA (n)[a]	DMAEA %	EA %	M_n[a] (g mol)	PDI[b]
P1	12	5	71	29	2387	1.19
P2	8	7	53	47	1958	1.16
P3	26	48	35	65	8893	1.21
P4	29	118	20	80	16373	1.18
P5	38	10	80	20	6975	1.20
P6	27	13	67	33	5546	1.15
P7	21	22	49	51	5504	1.22
P8	102	210	32	68	35604	1.17
P9	39	90	30	70	15141	1.11
P10	43	49	47	53	11665	1.13
P11	401	421	49	51	99515	1.15
P12	101	87	54	46	24588	1.12
P13	128	66	66	34	26730	1.11
P14	232	0	100	0	32300	1.28
P15	0	222	0	100	22200	1.17
BP1	78	26	75	25	13768	1.20
BP2	56	51	52	48	13118	1.22
BP3	20	56	26	74	8463	1.18
BP4	96	30	76	24	16745	1.17
BP5	112	61	67	35	22136	1.19

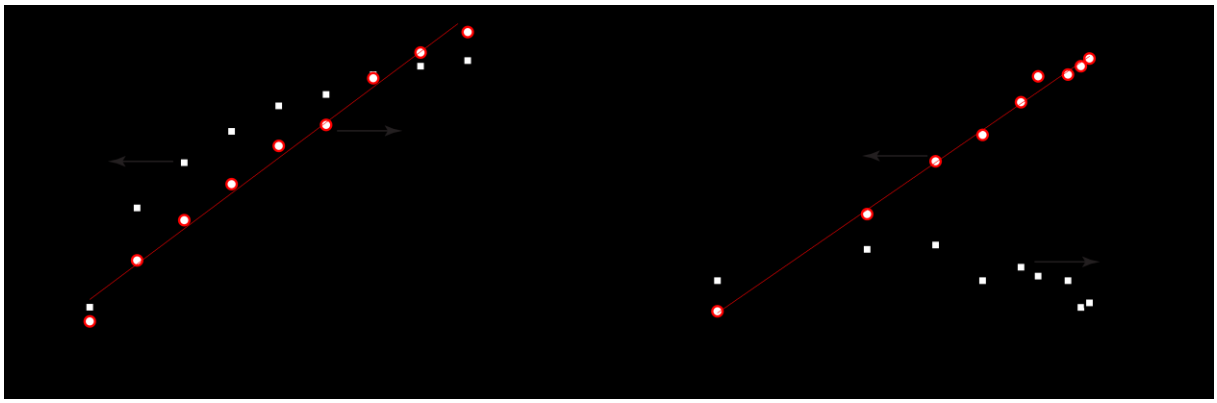

Figure 1. Analysis of conversion of DMAEA over time in the SET-LRP for the preparation of P5. Reaction condition: [DMAEA] : [EA] : [initiator] [Cu(0)]: [ligand] = 75 : 25 : 1: 1 : 0.1 in DMSO at 25 ºC. a) Conversion (black squares) and ln([M_0]/[M]) (red circles) vs. time, where [M_0] is the concentration of DMAEA at t=0; b) M_n (red circles) and PDI (black squares) vs. conversion.

Figure 2. Examples of ^{1}H NMR spectra (D_6-DMSO) of p(EA-co-DMAEA) random copolymers: P6 upper), P5 (middle), P1 (lower).

Table 2. Cell density on the polymers synthesized in this study (n=3).

Polymer	HeLa		HEK	
	Cell density / mm^2	SD	Cell density / mm^2	SD
P1	9	5	54	45
P2	9	5	140	2
P3	10	5	38	5
P4	14	6	159	20
P5	31	30	135	62
P6	42	25	183	1
P7	37	21	200	86
P8	150	59	401	94
P9	85	17	267	118
P10	76	52	626	128
P11	175	1	360	35
P12	14	6	119	27
P13	37	11	155	51
P14	79	30	483	111
P15	256	61	421	42
BP1	163	10	445	226
BP2	63	1	118	61
BP3	125	54	192	51
BP4	184	95	379	183
BP5	62	10	329	10

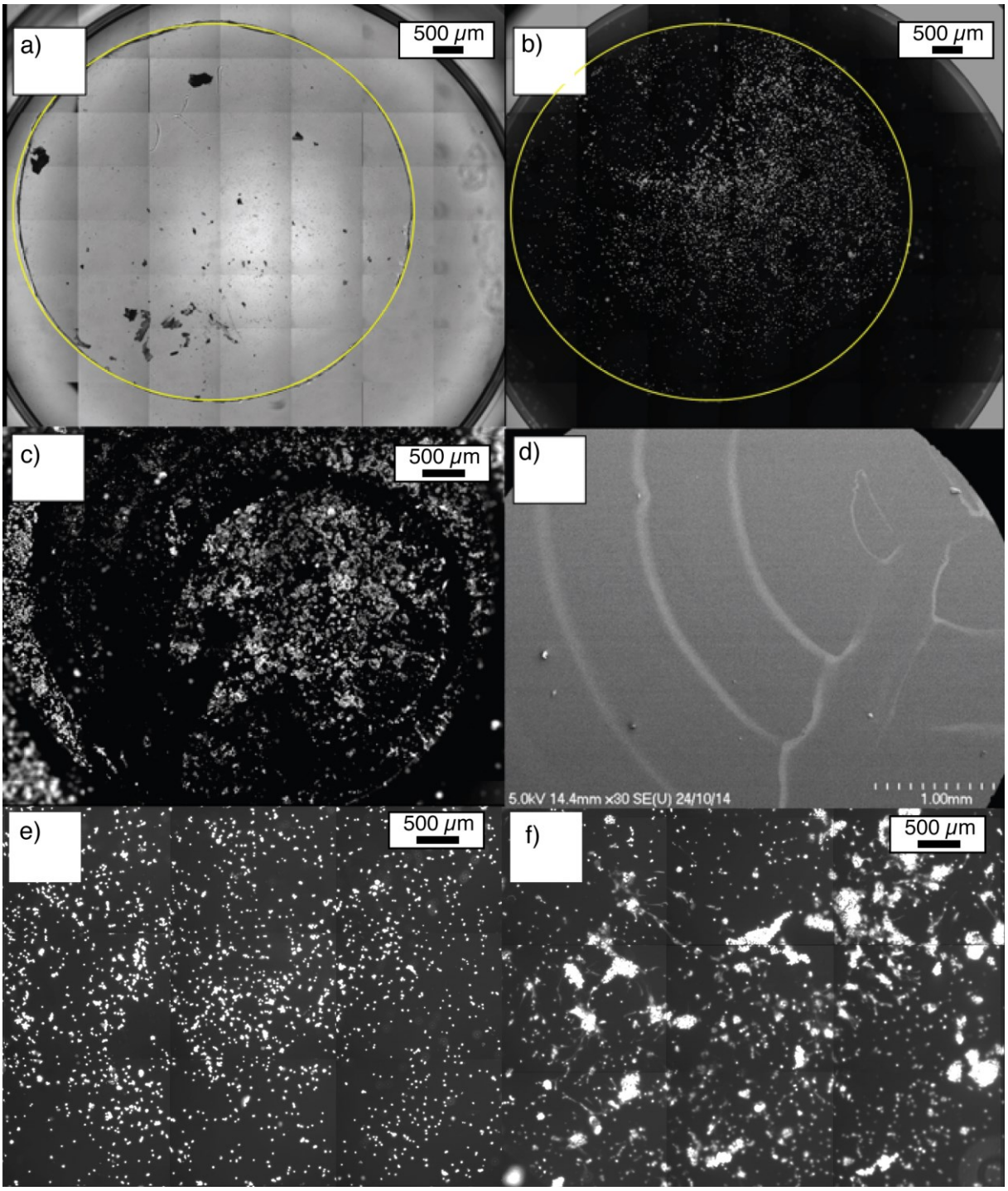

Figure 3. Images for polymer P12 seeded with HEK cells in a) bright-field channel and b) DAPI channel. The yellow circles indicate the areas of the glass coverslips scanned and used to calculate cell number. The software was set up to count the stained nuclei within the yellow circular area. Counting was performed using ImageJ plugin ITCS with cell nuclei detection defined by three parameters (nuclei width of 7 pixels, minimum distance between nuclei of 2.5 pixels and a threshold of 2.0 pixels). c) Images showing the cells attach according to the

topography of the polymer P14 surface when comparing to the d) SEM image of the polymer P14 coated coverslip. Fluorescence image of cells attachment on e) polymer P4 surface where cells evenly distributed over the coverslip and f) P14 surface where polymer promoted clumping. Scale bars: 500 µm.

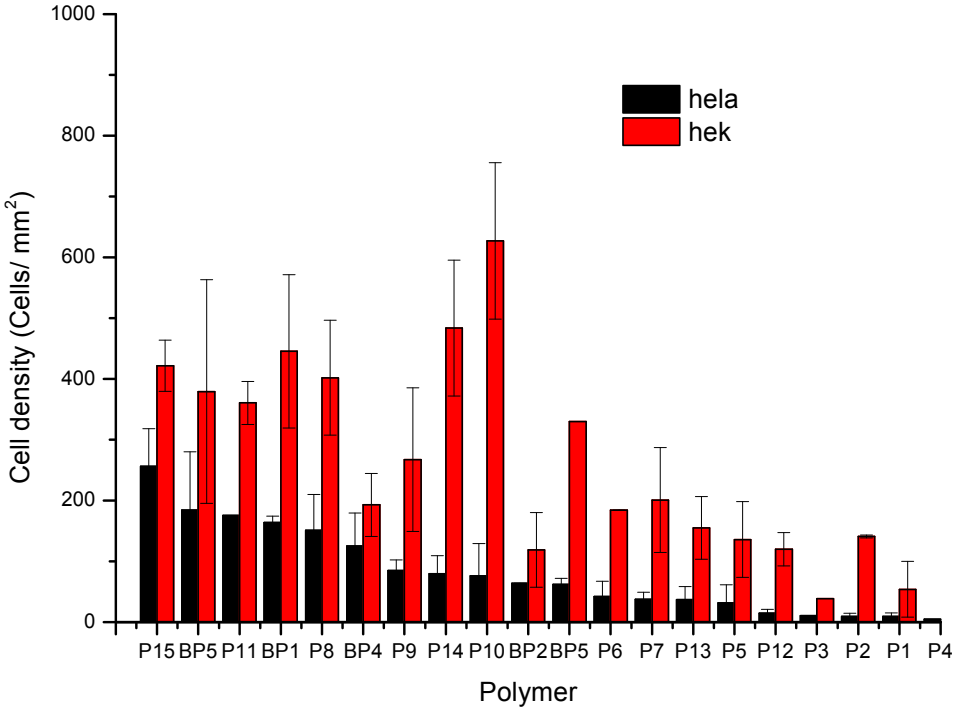

Figure 4. Graphs of density of HeLa cells and HEK cells on polymer coated coverslip. Error bars are standard deviation (n=3).

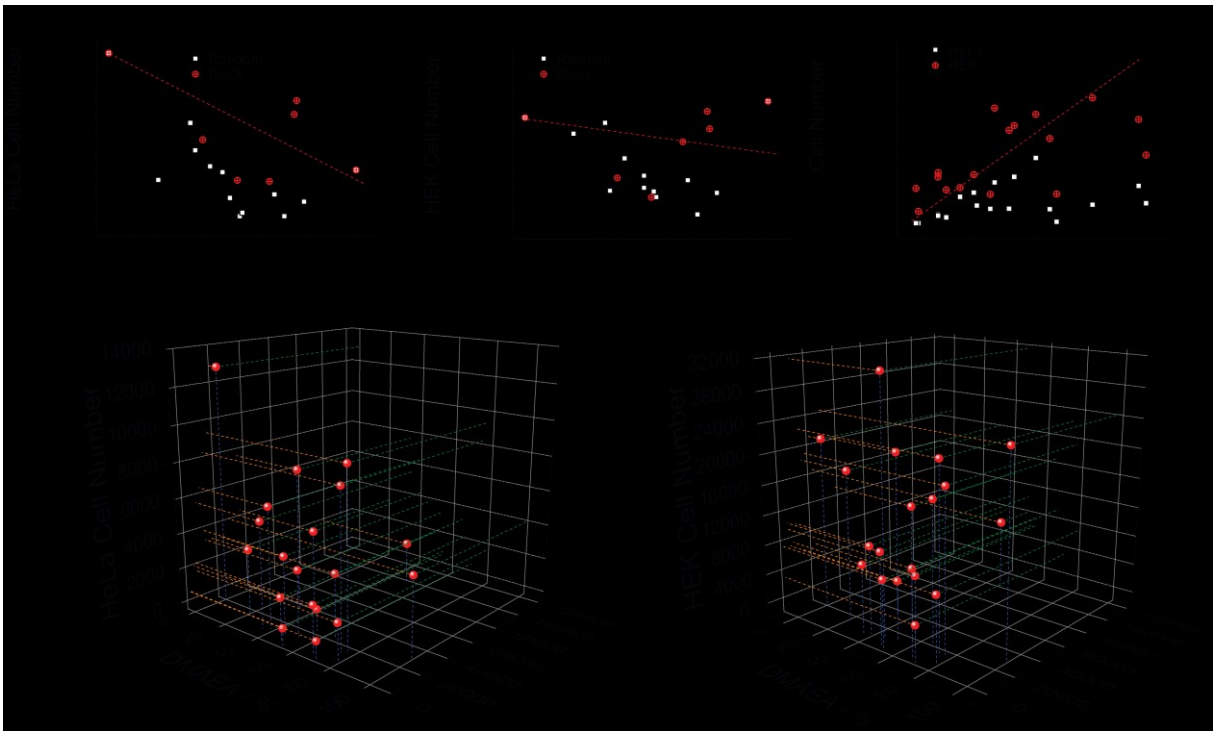

Figure 5. Correlation of HeLa and HEK binding with the percentage of DMAEA and polymer molecular weight (g.mol^{-1}, M_n): a) HeLa vs. DMAEA%; b) HEK vs. DMAEA%; c) HeLa and HEK vs. M_n; d) HeLa vs. DMAEA% vs. M_n (all the polymers); e) HEK vs. DMAEA% vs. M_n (all the polymers).

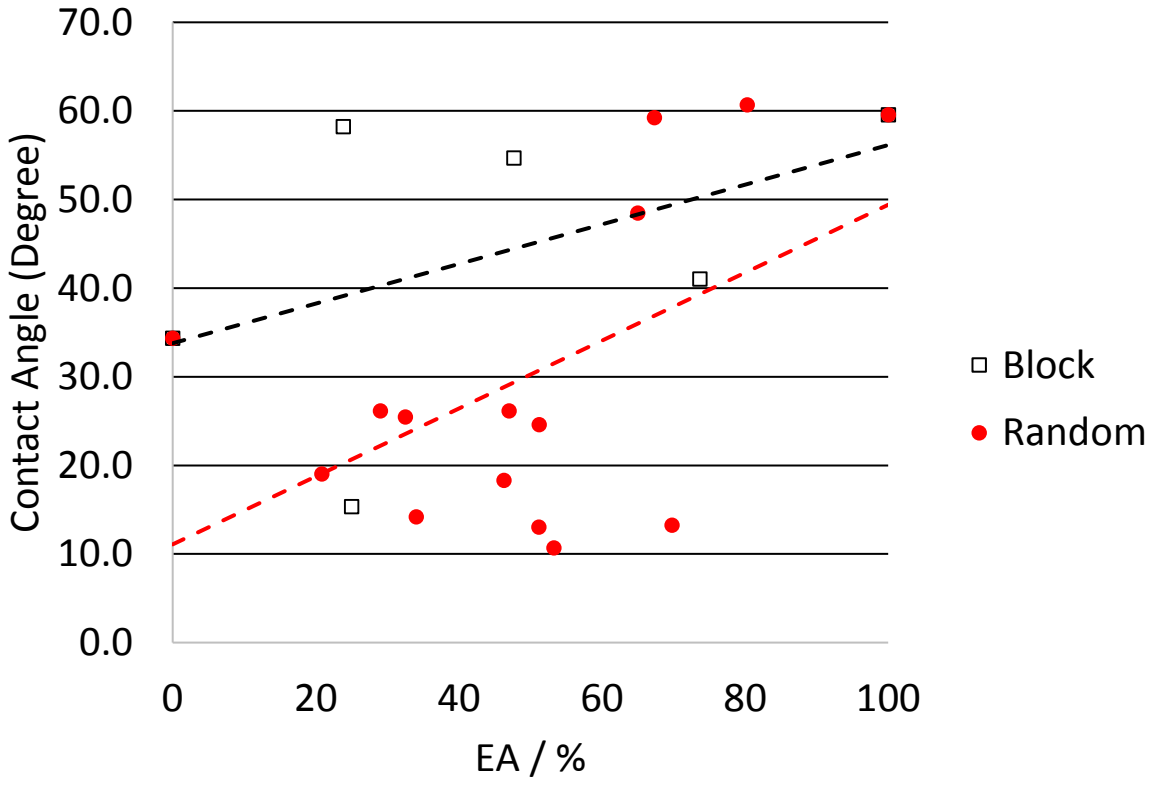

Figure 6: Correlation of block and random copolymer with contact angle measured on coverslips coated polymer surfaces.

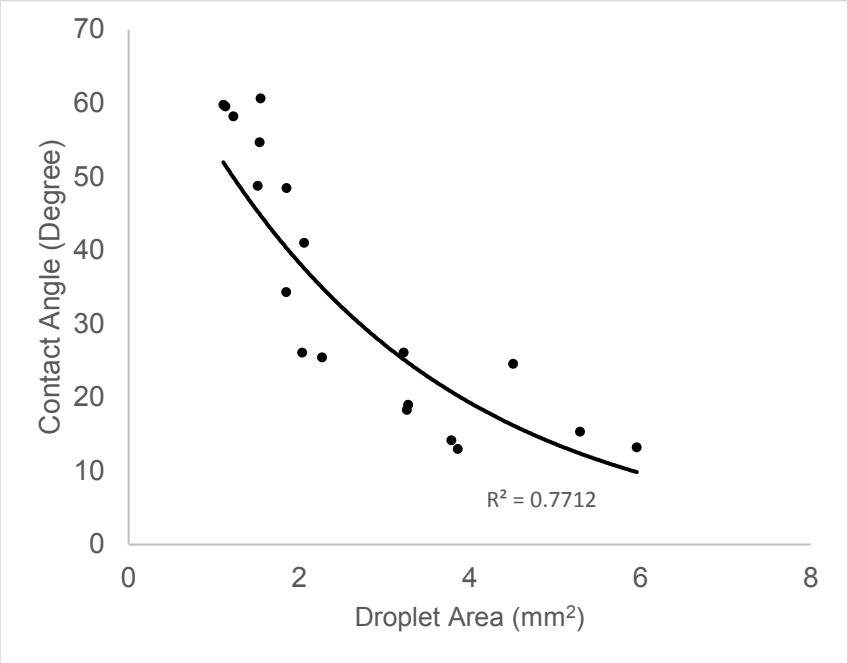

Figure 7. Spreading area versus contact angle.

Abstract for TOC:
Well-defined random and blcok copolymers from SET-LRP were examined for their performance in the attachment and growth of HeLa and HEK cells. The correlations between cellular attachment and the monomer composition as well as polymer chain length were observed.

((Supporting Information should be included here for submission only; for publication, please provide Supporting Information as a separate PDF file.))

Supporting Information

Table S1. Cell numbers on the polymers synthesized in this study (n=3).

Polymer	HeLa		HEK	
	Cell Number	SD	Cell Number	SD
P1	468	289	2716	2310
P2	474	271	7082	106
P3	5479	456	7225	725
P4	3233	234	18128	2234
P5	1572	1515	6824	3128
P6	2124	1260	9243	19
P7	1884	589	10088	4343
P8	7570	1965	20195	4739
P9	4270	883	13420	5934
P10	3829	650	31487	4997
P11	8801	141	18116	1774
P12	734	335	6014	1386
P13	1861	1077	7790	2580
P14	3984	1512	24302	6692
P15	12873	3104	21185	2114
BP1	8215	545	22374	2360
BP2	3200	212	5967	3083
BP3	6289	2720	9686	2600
BP4	9266	1812	19052	9227
BP5	3119	506	16564	2345

To gain insight into the correlation between the EA ratio on the polymer and the amount of cells adhered to the polymer surface cell seeding on coverslips was repeated twice with two independent sets of polymers (experiment 2 and experiment 3). The first set was comprised of 10 polymers (P1, P3, P4, P15, BP2, BP3, BP4, BP5, P12 and P14) in triplicate and a second set was composed of 8 polymers (P1, P3, P4, BP1, P15, BP5, P12, P14) in triplicate. In both cases similar trends of both HeLa and HEK binding on polymers surfaces were observed.

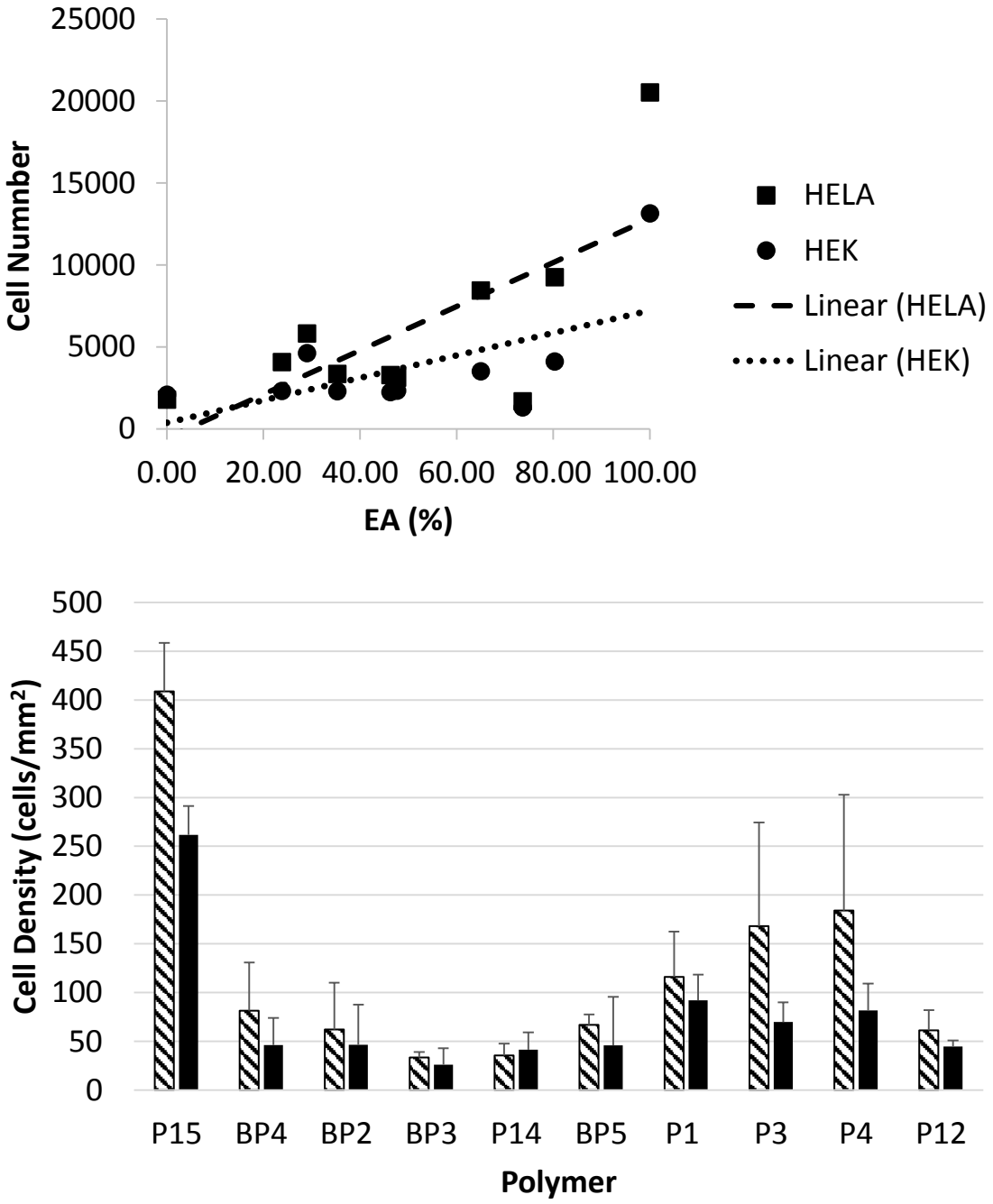

Figure S1. Experiment 2: correlation of HeLa and HEK bindings with percentage of EA. Error bars are standard deviation (n=3).

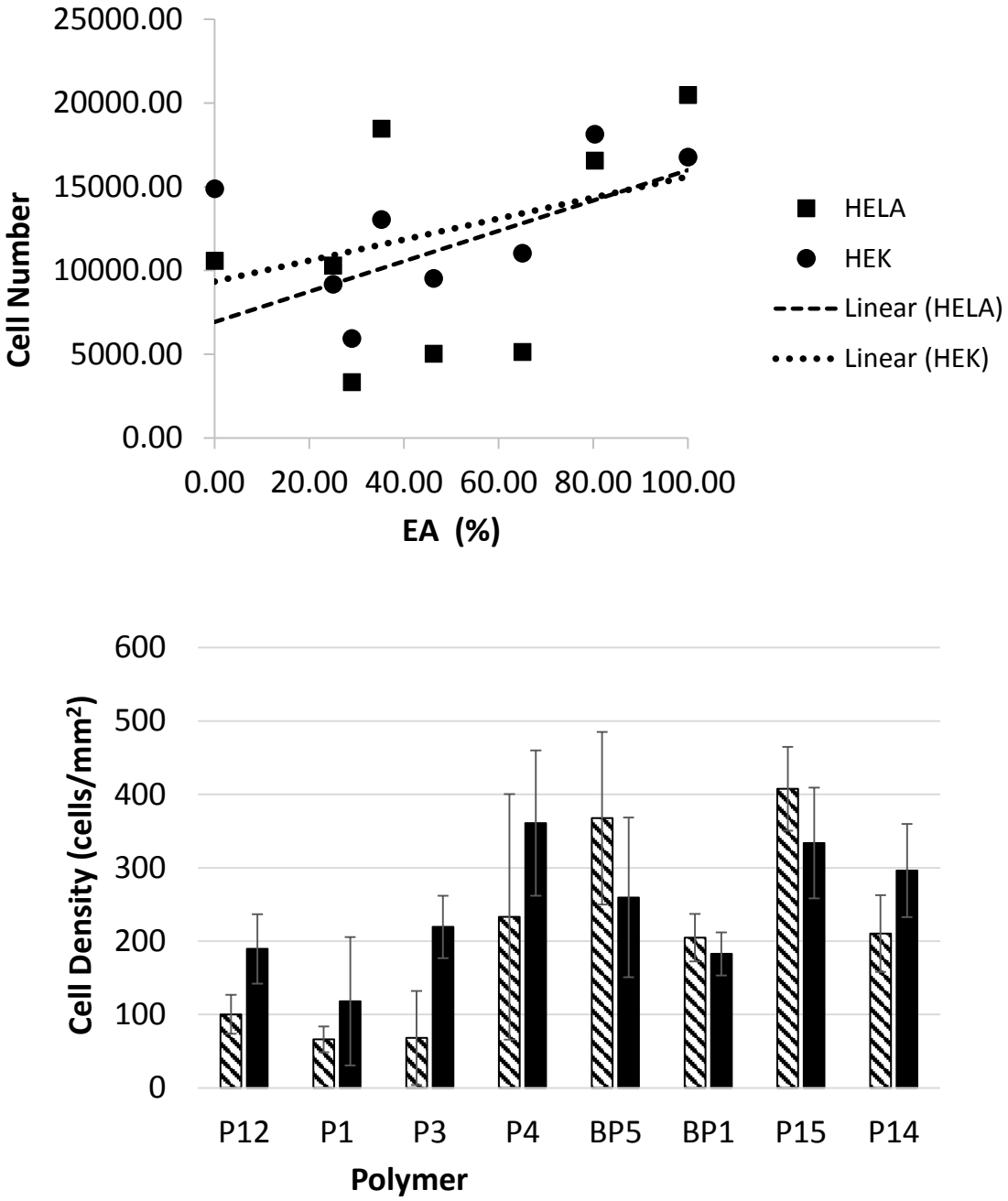

Figure S2. Experiment 3: correlation of HeLa and HEK bindings with percentage of EA. Error bars are standard deviation (n=3).

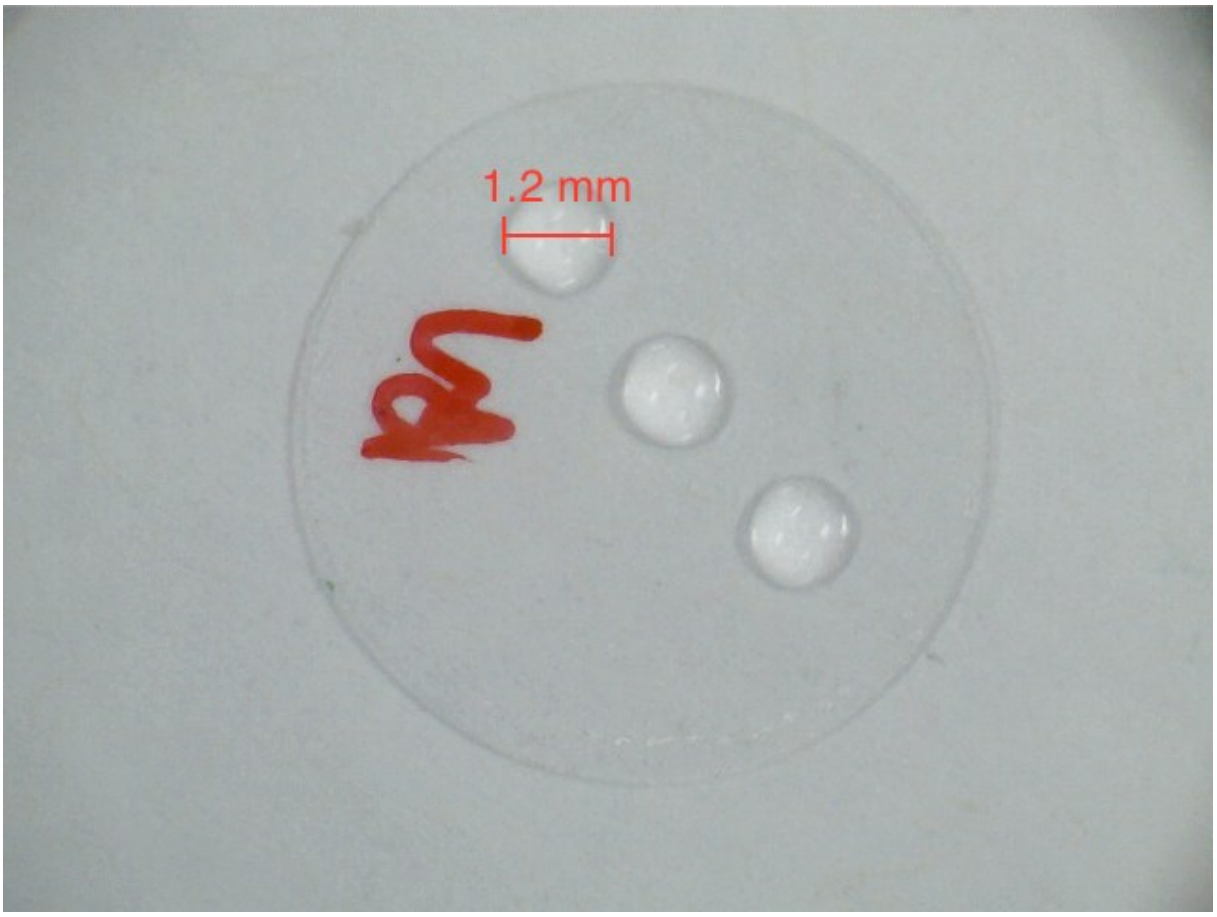

Figure S3. Images of water droplets on polymer film (P15). Diameter of the droplet was measured by ImageJ (d = 1.2 mm in the picture) and spreading area was then calculated using the equation: area = πr^2.

Table S2. Contact angle measurement (n = 9) and standard deviation on polymer coated coverslips.

CODE	Average Contact Angle	Standard Deviation
P1	26.11	2.96
P2	26.11	0.87
P3	48.44	3.69
P4	60.67	4.14
P5	19.00	1.83
P6	25.44	1.77
P7	13.00	1.94
P8	59.22	3.36
BP1	15.33	2.05
P9	14.17	1.21
P15	59.56	2.45
BP2	54.67	3.37
BP4	41.00	10.12
BP5	58.22	1.55
P11	13.22	1.13
P10	10.67	0.94
P13	24.56	1.95
P12	18.29	1.28
P14	34.33	5.40